Quantum Electronics **51** (11) 1038–1043 (2021)

LASER APPLICATIONS AND OTHER TOPICS IN QUANTUM ELECTRONICS https://doi.org/10.1070/QEL17646

Use of dielectric nanoparticles doped with Yb^{3+} ions to enhance the thermal effect in a biological tissue exposed to near-IR laser radiation (*in vivo* experiments)

P.A. Ryabochkina, S.A. Khrushchalina, A.N. Belyaev, O.S. Bushukina, I.A. Yurlov, S.V. Kostin

Abstract. **The conditions for the appearance of broadband radiation from particles of zirconium dioxide stabilised by ytterbium oxide upon excitation by intense laser radiation with a wavelength of 980 nm are investigated. It is shown that this radiation is observed at a lower excitation power density and lower ytterbium content than in particles of orthophosphates and their hydrates. As a result of *in vivo* experiments, the possibility of using ytterbium-containing particles to enhance the thermal effect from exposure to laser radiation with a wavelength of 980 nm on the skin of a rat is demonstrated.**

Keywords: *nanoparticles, rare-earth ions, effect of laser radiation on biological tissue.*

1. Introduction

The appearance of broadband 'white' radiation in nanoparticles under the action of intense laser radiation has been repeatedly reported in the scientific literature. Most publications are devoted to the study of this phenomenon in dielectric nanoparticles doped with rare-earth (RE) ions [1–16]. The authors of these papers have different points of view on the nature of such radiation. A significant part of researchers believe that it is thermal [2, 5–7, 15, 16]. We carried out our own investigations of nanosized oxide and fluoride compounds heavily doped with rare-earth ions (Yb^{3+}, Er), which confirm the thermal nature of the observed radiation [17–21]. We also proposed a mechanism responsible for the heating of particles to high temperatures upon their excitation in the absorption bands of rare-earth ions [17, 18, 20, 21]. In our opinion, this mechanism is based on the nonlinear interaction of rare-earth ions with each other and with structural defects. Because of this interaction, both the upper energy states of rare-earth ions and the levels of defects located near the bottom of the conduction band can be populated. With an increase in temperature, electrons from these levels pass to the conduction band. When electrons interact with phonons of the crystal lattice, dielectric particles are heated, as a result of which broadband 'white' radiation is observed.

According to the proposed mechanism, the conditions for the emergence of broadband 'white' radiation will depend on factors such as the concentration of rare-earth ions and their absorption coefficient at the excitation wavelength, the band gap of the material, and the number of defects in its structure. In Ref. [21], using the example of CaF_2, ZrO_2, as well as YVO_4 and YPO_4 particles with the same content of Er^{3+} ions, it was shown that in particles with a smaller band gap ($Y_{0.75}Er_{0.25}VO_4$) and a larger number of defects (ZrO_2 – 25 mol% Er_2O_3), thermal radiation occurs at a lower power density of the exciting radiation with a wavelength of 1550 nm.

Studies of the described phenomenon are not only of fundamental importance, but can also be of interest from a practical point of view. As noted above, the appearance of 'white' radiation in nanoparticles (NPs) doped with rare-earth ions, when excited in the absorption bands of these ions by intense laser radiation, is associated with the heating of particles to high temperatures. In Refs [21, 22], we hypothesised a possibility of applying this effect, e.g., in dermatology, to remove neoplasms. One of the methods currently used for this purpose is exposure to near-IR laser radiation [23–34], in particular, with a wavelength of about 980 nm [25–27, 29–34]. In this case, optical fibre is often used to deliver radiation to biological tissue, which makes it possible to implement both noncontact and contact methods of exposure [23–34]. To enhance the thermal effect in the contact method and increase the efficiency of the procedure, a number of authors propose a modification of the fibre tip, namely, the inclusion of strongly absorbing impurities in its composition [27–29], which makes it difficult to reuse the fibre. Preliminary coating of biological tissue with NPs capable of intense heating under the action of laser radiation can become an alternative way to increase the thermal effect upon contactless exposure. In addition, this method will reduce the power of the supplied laser radiation (up to 1–2 W) and, consequently, the cost of the operation.

As mentioned above, one of the types of compounds for which thermal radiation was observed were particles of zirconium dioxide stabilised with erbium oxide [21]. Compounds of this type have a number of important features, one of which is their bioinertness. Another distinctive feature of ZrO_2–M_2O_3 solid solutions (where M = Y or a rare-earth ion) is the presence of defects in the structure (oxygen vacancies) resulting from the heterovalent substitution of Zr^{4+} ions by Y^{3+} ions or trivalent rare-earth ions [35–42]. In our opin-

P.A. Ryabochkina, S.A. Khrushchalina, A.N. Belyaev, O.S. Bushukina, I.A. Yurlov, S.V. Kostin Ogarev Mordovia State University, Bol'shevistskaya ul. 68, 430005 Saransk, Russia; e-mail: ryabochkina@freemail.mrsu.ru

Received 20 July 2021; revision received 29 August 2021
Kvantovaya Elektronika **51** (11) 1038–1043 (2021)
Translated by V.L. Derbov

ion, it is the presence of structural defects that led to the fact that the minimum concentration of rare-earth ions in these particles, for which thermal radiation was observed, was lower than in other compounds [21]. The listed features allow considering the $ZrO_2-M_2O_3$ compounds (with M = Y, rare-earth ions) as promising candidates for the aforementioned application in biomedicine. Yb^{3+} ions can serve as doping ions, since they have effective absorption in the 980 nm region. In addition, as shown in [1, 2, 5, 7, 19, 20], for compounds doped with these ions, broadband thermal radiation also occurs.

The objectives of this work are to study the conditions for the appearance of broadband 'white' radiation in particles of zirconium dioxide stabilised by ytterbium oxide, when they are excited by laser radiation with a wavelength of 980 nm. We also study the possibility of enhancing the thermal contactless effect of laser radiation with this wavelength on biological tissue preliminarily coated with the NPs mentioned above.

2. Materials and methods

The ZrO_2-x mol% Yb_2O_3 nanoparticles (x = 5–50) were synthesised under hydrothermal conditions by the coprecipitation method [21]. The starting reagents were $ZrO(NO_3)_2\cdot 5H_2O$ (Reakhim, pure grade), $YbCl_3\cdot 6H_2O$ (Vekton, 99.9%), and NH_4OH (Lenreaktiv, analytical grade). For synthesis under hydrothermal conditions, an aqueous solution of a mixture of zirconium salts and ytterbium chloride (the content of ytterbium chloride varied in the range of 5–50 mol%) was dropped with stirring to a 25% aqueous solution of ammonia. The solution obtained after dropping was aged for 1 h at a temperature of 90 °C. After thermal treatment on a magnetic stirrer, the resulting mother liquor was washed three times using a centrifuge and dried in an oven at 90 °C for 24 h. After drying, the precipitate was ground in a porcelain mortar and annealed at 1000 °C for 4 h.

X-ray phase analysis of the samples was carried out using an Empyrean diffractometer (PANalitical B.V.) (CuK_α radiation, λ = 1.5414 Å) with a vertical goniometer and a PIXcel 3D detector. Particle sizes were controlled by dynamic light scattering using a NANOflex Microtrac analyser (operating range 0.8–5500 nm).

Studies of the spectral luminescent characteristics were carried out using an automated setup based on an MDR-23 monochromator. The excitation source was a semiconductor laser diode (λ_{exc} = 980 nm). The laser radiation power was monitored with a Standa 11 PMK30H-H5 Power Detector. The diode radiation was focused on the sample using a lens; the waist diameter, measured by the knife-edge scanning method [43, 44], was 360 μm. The power density of laser radiation was calculated as the ratio of its power after passing through the lens to the cross-sectional area of the beam at the lens focus. A FEU-79 photomultiplier was used as a radiation detector. All measurements were carried out at room temperature. The emission spectra were corrected for the spectral sensitivity of the setup. The colour temperature of the radiation was estimated by the spectral pyrometry method, described in Ref. [45], from the radiation spectra corrected for the spectral sensitivity of the setup.

For *in vivo* experiments, four adult white male Wistar rats weighing 180–220 g were selected as experimental animals. Before the start of the experiment, the animals were injected with combined anaesthesia (Zoletil + Xyla in a dosage of 0.1 mL per 100 g body weight) in accordance with the Declaration of Helsinki on the Humane Treatment of Animals (2000); and the Guidelines of an Ethics Committee Examining Biomedical Research (WHO, 2000). The animals were fixed in a prone position on a motorised stage (Zaber Technologies Inc.) with the possibility of precise displacement. A 4 × 3 cm area was shaved on the back of each rat, after which six areas 2 × 1 cm each were marked on it with a marker (Fig. 1). The semiconductor laser diode mentioned above was used as a radiation source. The radiation from the diode was focused onto the skin surface using the same lens that was used for spectroscopic measurements. For comparative analysis, point exposure (15 points per area: three rows of five points, distance between points in a row 3 mm, distance between rows 2.5 mm) was carried out both on the skin areas previously covered with particles (B, F), and on areas without preliminary application of particles (A, E). In this case, a layer of powder weighing 200 mg was applied to the corresponding areas of the skin with an area of 2 cm^2. The thickness of the powder layer was estimated based on its volume and was about 400 μm. The parameters of exposure to the skin areas are shown in Fig. 1.

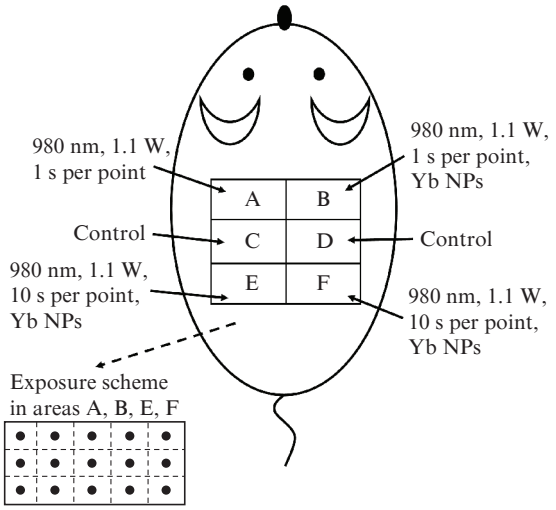

Figure 1. Scheme of the action of laser radiation with λ_{exc} = 980 nm and J = 865 W cm^{-2} on the rat back skin without coating (areas A and E) and previously coated with NPs (Yb NPs, areas B and F). In the lower left corner, a diagram of the location of points in areas A, B, E, F, on which the laser radiation was focused, is shown.

Experiments on animals were carried out in accordance with the provisions of the European Convention for the Protection of Vertebrate Animals used for Experimental and Other Scientific Purposes (Strasbourg, 1986) [46], the directive of the European Society (86/609/EEC) [47] and the Declaration of Helsinki. The keeping of animals and all experimental manipulations were carried out in accordance with the 'Rules for carrying out work with the use of experimental animals' (Order of the Ministry of Higher Education of the Russian Federation No. 724 of 11/13/1984).

The dynamics of skin wound healing was assessed on the 3rd, 7th, 10th, 20th, 27th, 35th day by the size of the wound, the presence of a scab, marginal or complete epithelialisation, and the formation of scar tissue.

3. Results and discussion

X-ray phase analysis of ZrO_2–x mol% Yb_2O_3 particles (x = 5–30) showed that they are single-phase and solid solutions with tetragonal (x = 5–10) [space group (SG) $P4_2/nmc$] [48] and cubic (x = 15–30) structures (SG $Fm3m$) [49] (Fig. 2). In particles with x = 50, along with the cubic phase (SG $Fm3m$), there is also a rhombohedral phase (SG $R\bar{3}$) [50]. The average size of the coherent scattering regions, estimated by the Scherrer formula, was 7 nm. Average particle sizes estimated by dynamic light scattering were 100–150 nm.

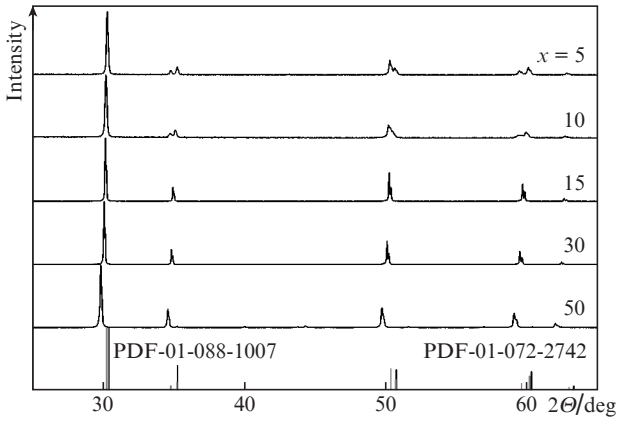

Figure 2. Diffraction patterns of concentration series ZrO_2–x mol% Yb_2O_3 (x = 5–50) (PDF-01-088-1007: tetragonal phase [46], and PDF-01-072-2742: cubic phase [47]).

Upon excitation of ZrO_2–x mol% Yb_2O_3 particles (x = 5–50) by cw laser radiation with λ_{exc} = 980 nm and power density J = 496 W cm^{-2} (P = 0.5 W) to the $^2F_{5/2}$ level of Yb^{3+} ions, the particles demonstrated luminescence of rare-earth ions, which are an uncontrolled impurity. An increase in J to 865 W cm^{-2} led to a significant change in the nature of particle radiation. The corresponding spectra are shown in Fig. 3a.

It follows from Fig. 3a that the emission spectrum of ZrO_2–5 mol% Yb_2O_3 particles is the spectrum of up-conversion luminescence of Ho^{3+} ions included in the sample as an uncontrolled impurity. These spectra are due to transitions from the excited multiplets $^5F_3$, $^5S_2$, $^5F_4$, and $^5F_5$ to the $^5I_8$ ground state, as well as from the $^5S_2$ level to the $^5I_7$ level of Ho^{3+} ions. These ions are excited both due to their direct absorption of radiation with λ_{exc} = 980 nm and due to nonradiative energy transfer from Yb^{3+} ions [51]. The appearance of up-conversion luminescence of Ho^{3+} ions in ZrO_2–5 mol% Yb_2O_3 particles upon excitation with J = 865 W cm^{-2}, as well as in particles with x = 10–50 at a lower excitation power density, indicates the presence of the interaction of rare-earth ions in the studied compounds.

Excitation of ZrO_2–x mol% Yb_2O_3 particles (x = 10–50) by cw laser radiation with λ_{exc} = 980 nm and J = 865 W cm^{-2} led to the appearance of broadband radiation in the range 400–780 nm (Fig. 3a). It is similar in shape to the profile of the emission spectra that we recorded earlier in NPs $Y_{0.95(1-x)}Yb_{0.95x}Er_{0.05}PO_4$, $YbPO_4$ [19], $Y_{0.95(1-x)}Yb_{0.95x}Er_{0.05}PO_4 \cdot 0.8H_2O$ (x = 0,3, 0,5, 0,7, 1), $YbPO_4 \cdot 0.8H_2O$ [20], $Y_{1-x}Er_xPO_4$, $Y_{1-x}Er_xVO_4$ (x = 0,25, 0,5, 0,75, 1) [17], ZrO_2–x mol% Er_2O_3 (x = 15, 25) [21], as well as the emission spectrum of a heated grey body (a TRSh-2850 tungsten lamp with a colour temperature of 2850 K). For clarity, the emission spectra of the particles and the tungsten lamp are shown in the inset in Fig. 3, and without taking into account the correction for the spectral sensitivity of the setup, the dip in the region 609–660 nm in these spectra is due to the peculiarities of the recording system. Based on this similarity, it can be concluded that the radiation of ZrO_2–x mol% Yb_2O_3 particles (x = 10–50) is also thermal. In this case, its colour temperature, estimated from the spectra, was 1910–2570 K, which is somewhat lower than the analogous values for particles of orthophosphates and orthophosphate hydrates containing Yb (2600–2700 K) [20]. It also follows from the spectra presented that 'white' radiation in particles of zirconium dioxide stabilised by ytterbium oxide occurs at a lower excitation power density and a lower content of ytterbium than in particles of orthophosphates and their hydrates. A similar trend was observed by us earlier for particles of ZrO_2–x mol% Er_2O_3 (x = 15, 25) [21] and $Y_{1-x}Er_xPO_4$ (x = 0.25–1) [17].

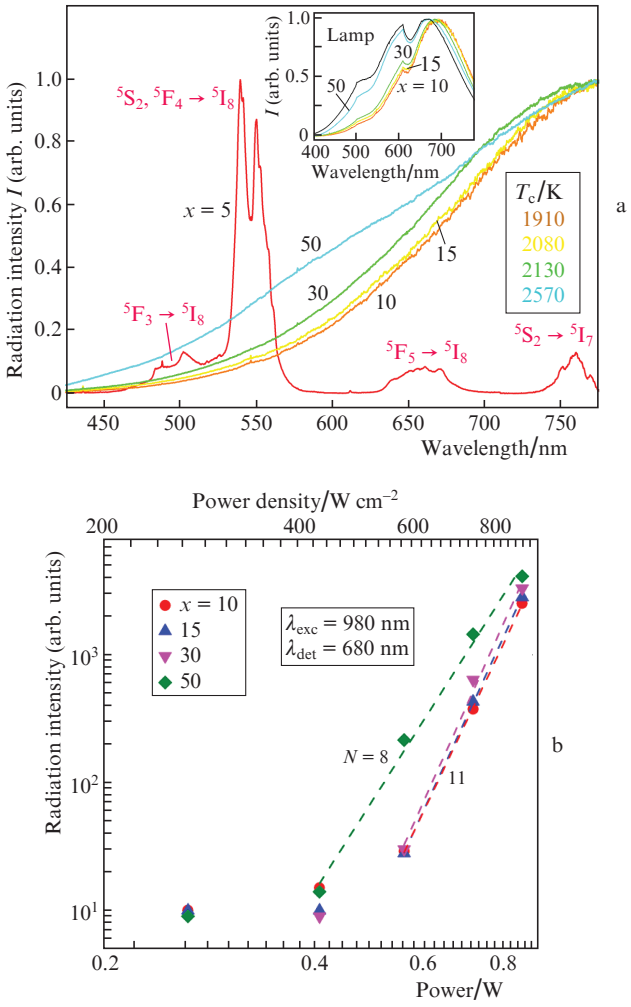

Figure 3. (Colour online) (a) Emission spectra of ZrO_2–x mol% Yb_2O_3 particles (x = 5–50) (λ_{exc} = 980 nm, J = 865 W cm^{-2}), taking into account the correction for the setup spectral sensitivity (the inset shows uncorrected emission spectra of these particles (x = 10–50) and the TRSh-2850 tungsten lamp with a colour temperature T_c = 2850 K) and (b) the intensity I of the broadband radiation of ZrO_2–x mol% Yb_2O_3 particles (x = 10–50) versus the exciting radiation power P (λ_{exc} = 980 nm) at a wavelength of 680 nm; $N$is the slope of the dependence $I(P)$.

Dependences of the intensity I of broadband radiation on the excitation power P for particles of $ZrO_2 - x$ mol% Yb_2O_3 ($x = 10-50$) were estimated at a wavelength of 680 nm and are shown in Fig. 3b in logarithmic coordinates. The wavelength for the measurements was chosen such that it did not coincide with the position of the luminescence band of the doping Yb^{3+} ions and corresponded to the region of high detector sensitivity. The slope N of the dependences $I(P)$ varies from 8 to 11 and exceeds the analogous values for orthophosphates ($N = 7.2$). As for the other particles listed above, such high values of N indicate the nonlinear nature of the dependence $I(P)$ and, together with the presence of a threshold value of the excitation power required for the appearance of 'white' radiation, may indicate the presence of avalanche-like processes [3, 17, 52].

Thus, a comparison of the characteristics and conditions for the occurrence of broadband 'white' radiation in ytterbium-containing zirconium dioxide particles with corresponding characteristics of orthophosphates revealed, on the one hand, general patterns; it is the shape of the contour of its spectrum, the nonlinear dependence of the intensity on the excitation power density, and a high colour temperature. On the other hand, for particles of $ZrO_2 - x$ mol% Yb_2O_3, a number of specific features were observed. Thermal radiation in $ZrO_2 - x$ mol% Yb_2O_3 compounds appeared at a lower content of RE ions ($x \geqslant 10$) than in $Y_{0.95(1-x)}Yb_{0.95x}Er_{0.05}PO_4$ ($x \geqslant 0.3$) [19]. In addition, for particles of zirconium dioxide stabilised with ytterbium oxide, the threshold value of excitation power density (420 W cm^{-2}) is lower than for orthophosphates (500 W cm^{-2}) with identical ytterbium content. These specific features are consistent with those described earlier for erbium-containing particles [21] and, in our opinion, are associated with a smaller band gap of the material and a higher concentration of defects in the structure. Thus, the results presented above indicate a large contribution of the interaction of defects to the process of electron delivery to the conduction band. As noted in the Introduction, the heating of NPs under the action of intense laser radiation described above can find practical application in biomedicine. To test this assumption, we carried out a series of *in vivo* experiments on the effect of laser radiation with $\lambda_{exc} = 980$ nm and $J = 865$ W cm^{-2} (0.88 W) on the surface of rat skin, both preliminarily coated with NPs and without coating. We selected ZrO_2–20 mol% Yb_2O_3 particles as samples for *in vivo* experiments.

Figure 4 shows photographs of rat skin areas obtained within 35 days from the beginning of the experiment. After a point exposure to laser radiation with $\lambda_{exc} = 980$ nm in areas A and E without preliminary application of NPs, there were small superficial epithelial wounds of a pale brown colour. In this case, the exposure time did not significantly affect the degree of damage. Much more pronounced skin lesions were detected in areas B and F, previously covered with NPs. Three days after the procedure, in area B with a short exposure time (1 s per point), there was a pale pink wound covered with delicate fibrin. In area F with a long exposure time (10 s per point), a dark wound covered with a skin scab and a layer of fibrin was noted. Certain difference in the shape of wounds from rectangular (corresponding to the geometry of the point impact) is due to the fact that the heat from each of the skin areas, on which the laser radiation was focused, spread uniformly in the radial direction [53], and the resulting surface damage had the shape of a circle. Due to the spread of heat beyond the focusing points and the small distance between them, the applied method of exposure to the skin led to the formation of wounds that formed a continuous damage. On the 10th day from the beginning of the experiment, the wound in area B as a result of edge epithelialisation decreased in size three to four times, and the rest of it became covered with a scab. The wound in area F was covered with a dry, grey-brown scab. At the edges of the wound, there was a pale pink strip of epithelialisation about 2 mm wide. On the 20th day, the wound in area B was completely epithelised and hair growth was noted. The wound in area F decreased in size due to marginal epithelialisation and scarring, the rest of it was covered with a dark pink scab. On the 32nd day, wounds in area F healed completely due to marginal epithelialisation and scarring. By this time, the rats had regenerated hair-covering.

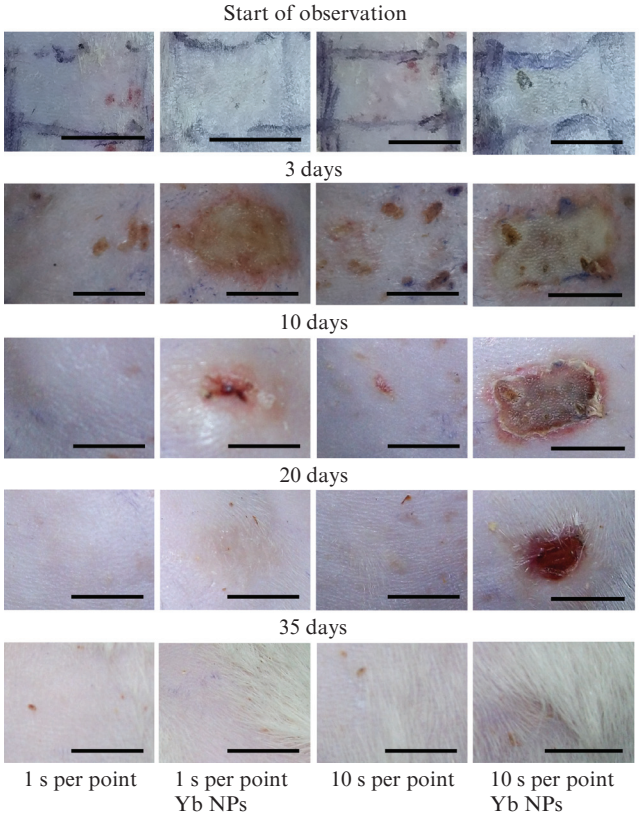

Figure 4. (Colour online) Dynamics of skin wound healing in rats after point exposure to laser radiation with $\lambda_{exc} = 980$ nm and $J = 865$ W cm^{-2} without coating and with preliminary application of NPs (Yb NPs). The scale corresponds to 1 cm.

Thus, a comparative analysis of the nature of the rat skin damage and the dynamics of its healing after exposure to laser radiation with $\lambda_{exc} = 980$ nm and $P = 0.88$ W showed that preliminary application of ZrO_2–20 mol% Yb_2O_3 particles leads to visually more pronounced damage and increases the period of wound healing by approximately 1.5–2 times. This analysis also allows estimating the depth of thermal damage. It is known that superficial wounds in rats (within the epidermis) heal within two weeks due to epithelialisation from the edges and bottom of the wound [54]. Deep wounds (with damage to the entire thickness of the

dermis) heal within four to five weeks in the form of marginal epithelialisation (for small wounds) or scarring. In our experiments, after short-time exposure to laser radiation (1 s per point) and preliminary coating with NPs (region B), superficial (within the epidermis) skin damage occurred, which independently epithelised within 20 days. An increase in the exposure time led to deep (within the dermis) damage to the skin, which healed by marginal epithelialisation within 32 days.

4. Conclusions

The study of the spectral and luminescent characteristics of zirconia particles stabilised with ytterbium oxide confirmed that the presence of defects in the material structure has a significant effect on the conditions for the appearance of thermal radiation in them upon excitation by intense laser radiation. In the course of *in vivo* experiments, it was demonstrated that preliminary deposition of ytterbium-containing NPs on the surface of biological tissue enhances the thermal effect from exposure to laser radiation with λ_{exc} = 980 nm. Under various parameters of the effect of laser radiation on the skin of rats without preliminary coating with NPs, changes occurred within the stratum corneum in the form of the formation of brown spots; the integrity of the epidermis was not violated. After exposure to laser radiation on the skin of rats, previously coated with NPs, pronounced wounds appeared on it. The degree of damage increased with increasing exposure time. To control the depth of thermal damage to biological tissue, further optimisation of such exposure parameters as radiation power and exposure time, as well as the volume of NPs applied to biological tissue, is required. In addition, further experiments on biological tissues with various neoplasms will reveal the dependence of the degree of damage on the type of tissue and give practical recommendations.

Acknowledgements. The authors are grateful to V.M. Kyashkin for help in the X-ray phase analysis of the samples.

This work was supported by the RF President's Grants Council (Grant No. MK-5500.2021.1.2) and partially by the Russian Foundation for Basic Research (Grant No. 19-32-90135).

References

1. Marciniak L., Strek W., Hreniak D., Guyot Y. *Appl. Phys. Lett*., **105**, 173113 (2014).
2. Redmond S.M., Rand S.C., Oliveira S.L. *Appl. Phys. Lett*., **85**, 5517 (2004).
3. Strek W., Marciniak L., Bednarkiewicz A., Lukowiak A., Wiglusz R., Hreniak D. *Opt. Express*, **19**, 14084 (2011).
4. Wang J., Tanner P.A. *J. Am. Chem. Soc*., **132**, 947 (2010).
5. Redmond S.M., Rand S.C., Ruan X.L., Kaviany M. *J. Appl. Phys*., **95**, 4069 (2004).
6. Bisson J.-F., Kouznetsov D., Ueda K.-I., Fredrich-Thornton S.T., Petermann K., Huber G. *Appl. Phys. Lett*., **90**, 201901 (2007).
7. Tabanli S., Cinkay Yilmaz H., Bilir G., Erdem M., Eryurek G., Di Bartolo B., Collins J. *ECS J. Sol. State Sci. Technol*., **7**, R3199 (2018).
8. Zhu Y., Xu W., Li C., Zhang H., Dong B., Xu L., Xu S., Song H. *Appl. Phys. Exp*., **5**, 092701 (2012).
9. Xu W., Min X., Chen X., Zhu Y., Zhou P., Cui S., Xu S., Tao L., Song H. *Sci. Rep*., **4**, 5087 (2014).
10. Xu S., Zhu Y., Xu W., Dong B., Bai X., Xu L., Miao C., Song H. *Appl. Phys. Express*, **5**, 102701 (2012).
11. Cinkaya H., Eryurek G., Di Bartolo B. *Ceram. Intern*., **44**, 3541 (2018).
12. Tomala R., Hreniak D., Strek W. *Opt. Mater*., **74**, 135 (2017).
13. Strek W., Marciniak L., Hreniak D., Lukowiak A. *J. Appl. Phys*., **111**, 024305 (2012).
14. Strek W., Tomala R., Marciniak L., Lukaszewicz M., Cichy B., Stefanski M., Hreniak D., Kedziorski A., Krosnickic M., Seijo L. *Phys. Chem. Chem. Phys*., **18**, 27921 (2016).
15. Bilir G., Di Bartolo B. *Opt. Mater*., **36**, 1357 (2014).
16. Silva Filho C.I., Oliveira A.L., Pereira S.C.F., de Sá G.F., da Luz L.L., Alves Júnior S. *Dalton Trans*., **48**, 2547 (2019).
17. Khrushchalina S.A., Ryabochkina P.A., Zharkov M.N., Kyashkin V.M., Tabachkova N.Yu., Yurlov I.A. *J. Lumin*., **205**, 560 (2019).
18. Khrushchalina S.A. Cand. Dis. (N. Novgorod: Lobachevsky Nizhny Novgorod State University, 2017).
19. Khrushchalina S.A., Ryabochkina P.A., Kyashkin V.M., Vanetsev A.S., Gaitko O.M., Tabachkova N.Yu. *JETP Lett*., **103**, 302 (2016) [*Pis'ma Zh. Eksp. Teor. Fiz*., **103**, 342 (2016)].
20. Khrushchalina S.A., Ryabochkina P.A., Kyashkin V.M., Vanetsev A.S., Gaitko O.M., Tabachkova N.Yu. *JETP Lett*., **103**, 743 (2016) [*Pis'ma Zh. Eksp. Teor. Fiz*., **103**, 836 (2016)].
21. Ryabochkina P.A., Khrushchalina S.A., Yurlov I.A., Egorysheva A.V., Atanova A.V., Veselova V.O., Kyashkin V.M. *RSC Adv*., **10**, 26288 (2020).
22. Khrushchalina S.A., Ryabochkina P.A., Belyaev A.N., Bushukina O.S., Yurlov I.A., Dvoryanchikova M.A., Kuznetsova O.A. *Mater. 17-oi Mezhdunar. nauchn. konf.-shk*. (Proc. 17th Int. Sci. Conf.) (Saransk: Publishing House of Mordovian University, 2018) p. 148.
23. Klein A., Umler W.B., Landthaler M., Babilas P. *Int. J. Hyperthermia*, **27**, 762 (2011).
24. Azadgoli B., Baker R.Y. *Ann. Transl. Med*., **4**, 452 (2016).
25. Stebbins W.G., Hanke C.W., Petersen J. *Dermat. Ther*., **24**, 125 (2011).
26. Wollina U. *Indian J. Dermatol*., **61**, 540 (2016).
27. Belikov A.V., Skrypnik A.V. *Lasers Surg. Med*., **51**, 185 (2019).
28. Belikov A.V., Skrupnik A.V., Kurnyshev V.Yu., Shatilova K.V. *Quantum Electron*., **46**, 534 (2016) [*Kvantovaya Elektron*., **46**, 534 (2016)].
29. Romanos G.E., Malhotra U., Tedesco R.W., Hou W., Delgado-Ruiz R. *Photomed Laser Surg*., **39**, 334 (2021).
30. Belikov A.V., Gelfond M.L., Shatilova K.V., Sosenkova S.A., Lazareva A.A. *Proc. SPIE*, **9542**, 95420J (2015).
31. Kassab A.N., El Kharbotly A. *Eur. Arch Otorhinolaryngol*, **269**, 419 (2012).
32. Derjabo A.D., Cema I., Lihacova I., Derjabo L. *Proc. SPIE*, **8803**, 88030B (2013).
33. Nammour S., El Mobadder M., Namour M., Namour A., Arnabat-Dominguez J., Grzech-Leśniak K., Vanheusden A., Vescovi P. *Int. J. Environ. Res. Public. Health*, **17**, 8665 (2020).
34. Pal M., Saokar A., Gopalkrishna P., Rajeshwari H.R., Kumar S. *Gen. Dent*., **68**, 28 (2020).
35. Kuzminov Yu.S., Lomonova E.E., Osiko V.V. *Tugoplavkie materialy iz kholodnogo tiglya* (Refractory Materials from a Cold Crucible) (Moscow: Nauka, 2004).
36. Pyatenko Yu.A. *Dokl. Akad. Nauk SSSR*, **173**, 634 (1967).
37. Nicoloso N., Lobert A., Leibold B. *Sens. Actuators B*, **8**, 253 (1992).
38. Wachsman E.D., Jiang N., Frank C.W., Mason D.M., Stevenson D.A. *Appl. Phys. A: Sol. Surf*., **50**, 545 (1990).
39. PaiVerneker V.R., Petelin A.N., Crowne F.J., Nagle D.C. *Phys. Rev. B*, **40**, 8555 (1989).
40. Ricca C., Ringuedé A., Cassir M., Adamoa C., Labat F. *RSC Adv*., **5**, 13941 (2015).
41. Li X., Mao X., Feng M., Xie J., Jiang B., Zhang L. *J. Eur. Ceram. Soc*., **36**, 418 (2016).
42. Foster A.S., Sulimov V.B., Lopez Gejo F., Shluger A.L., Nieminen R.M. *Phys. Rev. B*, **64**, 224108 (2001).
43. Suzaki Y., Tachibana A. *Appl. Opt*., **14**, 2809 (1975).
44. Brost G., Horn P., Abtahi A. *Appl. Opt*., **24**, 38 (1985).
45. Magunov A.N. *Instrum. Exp. Tech*., **52** (4), 451 (2009) [*Prib. Tekh. Eksp*., (4), 5 (2009)].

46. *European Convention for the Protection of Vertebrate Animals used for Experimental and other Scientific Purposes (ETS N 123)* (Strasbourg, 18.03.1986).
47. Directive 2010/63/EU of the European Parliament and of the Council of 22 September 2010 on the Protection of Animals Used for Scientific Purposes. *Off. J. Europ. Union*, **L276**, 33 (2010).
48. Malek J., Benes L., Mitsuhashi T. *Powder Diff*., **12**, 96 (1997).
49. Katz G. *J. Am. Ceram. Soc*., **54**, 531 (1971).
50. Thornber M.R., Bevan D.J.M. *J. Sol. State Chem*., **1**, 536 (1970).
51. Pandey A., Rai V.K., Dey R., Kumar K. *Mat. Chem. Phys*., **139**, 483 (2013).
52. Auzel F. *Chem. Rev*., **104**, 139 (2004).
53. Iizuka M.N., Vitkin I.A., Kolios M.C., Sherar M.D. *Phys. Med. Biol*., **45**, 1335 (2000).
54. Popov N.S., Demidova M.A., Shestakova V.G., Eliseeva T.I., Kazaishvili Yu.G. *Verkhnevolzhskii Med. Zh*., (12), 45 (2014).